THE AERONAUTICAL QUARTERLY

A JOURNAL DEVOTED TO AERONAUTICS AND THE ALLIED SCIENCES

Volume XXIII November 1972 Part 4

CONTENTS

ROYAL AERONAUTICAL SOCIETY
4 HAMILTON PLACE, W1V 0BQ
LONDON

The Pressure on Flat and Anhedral Delta Wings with Attached Shock Waves

J PIKE

(Royal Aircraft Establishment, Bedford)

Summary: An expression is derived which relates the pressure on a wing in a supersonic free stream to the pressure on a thin wing with the same surface shape. The expression is used to find the pressure distribution for caret wings and flat delta wings with attached flow at their leading edges. The compression surface pressure distributions found are in good agreement with existing experimental and theoretical results, except when large pressure changes occur in the flow behind the attached shock wave. Some expansion surface results are also obtained for wings with an isentropic expansion at the leading edge. The effects of flow and geometry changes on the pressure distribution are investigated. It is found that a small improvement in the lift/drag ratio of a caret wing can be obtained by halving the anhedral required for the plane shock wave condition.

1. Introduction

For thin wings which cause only a small disturbance to a supersonic free stream, the well-known linear theory of supersonic flow can be used to predict the pressure distribution over the wing. For wings which cause a strong disturbance in the flow linear theory is not usually adequate, and other means of estimating the pressures must be sought. Often much of the strong disturbance occurs as a discontinuous change across a shock wave, leaving behind the shock wave comparatively weaker disturbances. In such cases the application of linear theory to the flow behind the shock wave may provide an accurate means of estimating the flow conditions.

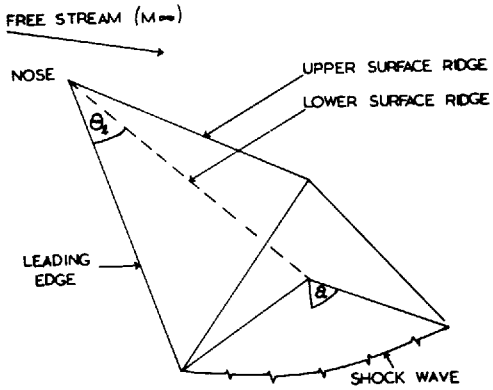

Figure 1 A caret wing

The technique is applied to caret wings[1] (Fig 1), which have the property that for certain combinations of Mach number and incidence they support a plane shock wave on their leading edge. The non-linear errors involved in perturbing this plane shock wave condition are reduced by constructing a non-dimensional pressure function in which cancellation of the non-linear terms occurs. The pressure function is found to give accurate results for a wide range of caret wings, including flat delta wings. A method of extending the technique to the upper surface of a caret wing and to diamond shaped wings is also given.

Notation

a half-angle between wing facets

b angle subtended at nose by a tangent from leading edge to Mach cone from nose

Received November 1971; revision received January 1972

M		Mach number
p		static pressure
p_w		wedge pressure at wing incidence and Mach number
p_l		leading edge pressure
t_1, t_2		defined by equations (3) and (4), respectively
a		incidence to free stream
β	=	$(M^2 - 1)^{1/2}$
γ		ratio of specific heats
δ		small incidence change
θ, ϕ		spherical polar coordinates based on wing nose and ridge line
θ_l		angle between leading edge and ridge line
λ		reflection coefficient of disturbance from shock wave
ω		angle between lower surface ridge line and leading edge plane

Suffix

r	reference flow conditions

2. The Thin Caret Wing

A thin caret wing at a small incidence δ to the free stream is shown in Figure 2. The wing is symmetrical about a vertical plane through OO′, and the geometry is described by θ_l = angle POO′ and 2a = angle PO′P′.

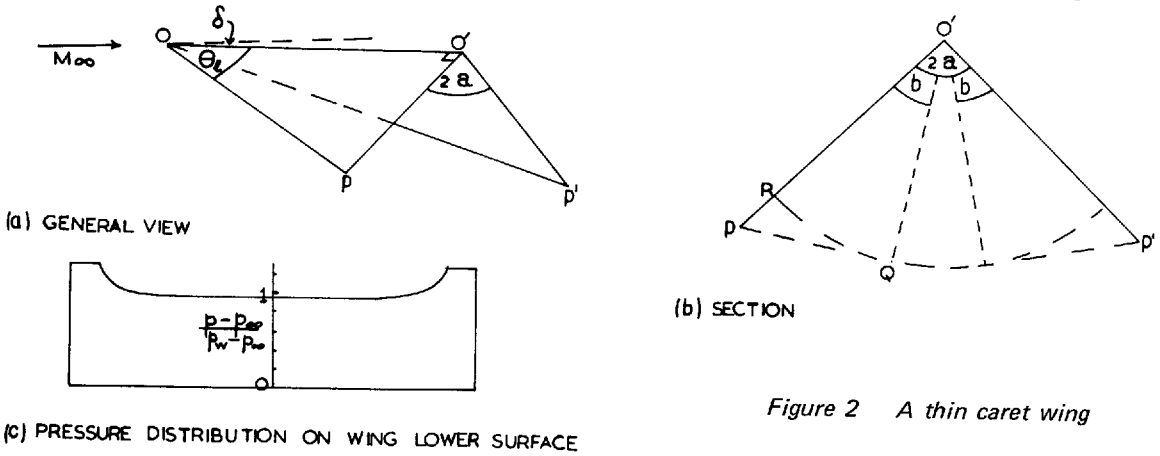

Figure 2 A thin caret wing

For supersonic leading edges (i.e. $\cot\theta_l < \beta_\infty$) a region bounded upstream by the Mach plane from the leading edge (PQ) and downstream by the Mach cone from the nose (QR) has constant pressure. Linear theory[2] gives this pressure as

$$p_l = p_\infty + \gamma p_\infty \frac{M_\infty^2}{\beta_\infty} \frac{\sin a}{\sin b} \delta, \tag{1}$$

where b is the angle subtended at the ridge line (OO′) by the tangent from the leading edge to the downstream Mach cone from the nose (i.e. b = angle PO′Q). For the pressure in the region downstream of the Mach cone, expressions have been derived[2] which for symmetrical wings reduce to

$$p = p_\infty + \gamma p_\infty \frac{M_\infty^2}{\beta_\infty} \frac{\sin a}{\sin b} \delta (t_1 + t_2), \tag{2}$$

where

$$t_1 = \frac{1}{\pi} \tan^{-1} \left\{ \frac{\tan[(b+\phi)\pi/2a]}{(1-\beta_\infty^2 \tan^2\theta)^{1/2}} \right\} \tag{3}$$

and

$$t_2 = \frac{1}{\pi} \tan^{-1} \left\{ \frac{\tan[(b-\phi)\pi/2a]}{(1-\beta_\infty^2 \tan^2\theta)^{1/2}} \right\}. \tag{4}$$

In equations (3) and (4) θ and ϕ are polar coordinates with $\theta = 0$ the line OO′ , $\theta = \cot^{-1}(\beta_\infty)$ the line OR , $\phi = 0$ the plane OO′P and $\phi = 2a$ the plane OO′P′ .

These equations are used to give the pressure distribution shown in Figure 2(c) for the wing of Figure 2(b).

As Q lies on the Mach cone from O , b and M_∞ are related by

$$\beta_\infty = \sec b \cot \theta_l . \tag{5}$$

Thus t_1 and t_2 can be written

$$t_1 = \frac{1}{\pi} \tan^{-1} \left\{ \frac{\tan[(b+\phi)\pi/2a]}{(1-\sec^2 b \cot^2 \theta_l \tan^2 \theta)^{1/2}} \right\} \tag{6}$$

$$t_2 = \frac{1}{\pi} \tan^{-1} \left\{ \frac{\tan[(b-\phi)\pi/2a]}{(1-\sec^2 b \cot^2 \theta_l \tan^2 \theta)^{1/2}} \right\} , \tag{7}$$

where a and θ_l are purely geometrical parameters and b is a flow parameter which may be evaluated either from the free-stream flow or the perturbed leading edge flow.

When b = a equations (1) and (2) reduce to

$$p_w = p_\infty + \gamma p_\infty \frac{M_\infty^2}{\beta_\infty} \delta , \tag{8}$$

where p_w is the pressure on a two-dimensional wedge at incidence δ .

3. Thick Caret Wings

The formulae of Section 2 use the free stream as a reference flow. However, similar formulae could be obtained for a small perturbation from any other reference flow, for example from a known flow whose boundary conditions are nearly the same as the flow to be determined.

The reference flow used here for the caret wing compression surface is the parallel flow behind a plane shock wave attached to the leading edges of the wing. The strength of this shock wave depends on the free-stream Mach number, the wing incidence and the single geometrical parameter ω defined as the angle between the lower surface ridge line and the leading edge plane. The parameter ω is related to θ_l and a by

$$\tan \omega = \tan \theta_l \cos a .$$

Consider typically a wing with $\omega = 20°$; then the incidence and free-stream Mach number combinations for which the wing supports a shock wave in the plane of the leading edges is shown in Figure 3(a). Suppose we wish to know the flow conditions at M = 2.8 and $\alpha = 15°$ as indicated by the cross in Figure 3(a). Then the flow could be treated as an incidence perturbation of the flow at M = 2.8 and $\alpha = 3.5°$ or a much smaller Mach

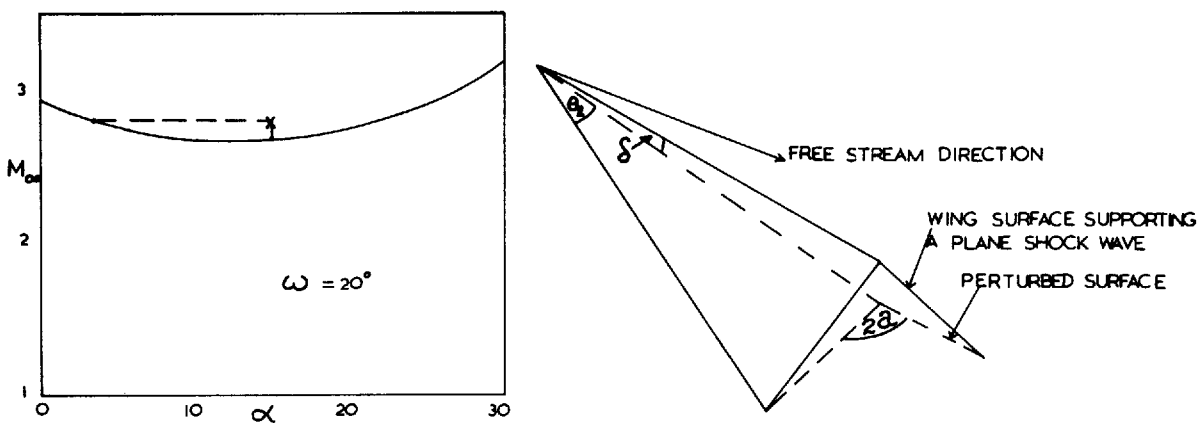

(a) PLANE SHOCK CONDITIONS FOR $\omega = 20°$ (b) PERTURBATION FROM PLANE SHOCK CONDITION

Figure 3 Perturbation of a wing supporting a plane shock wave

number perturbation of the flow at $M = 2.67$ and $\alpha = 15°$. If ω were to be taken as the third axis in Figure 3(a), then the curve shown would be the intersection of the $\omega = 20°$ plane with the surface representing all the conditions for which the wing supports a plane shock wave. Thus the conditions at the point shown by the cross could also be obtained by keeping M and α constant and perturbing the shape. It is found that a combination of shape and incidence perturbation which leaves the leading edge unaffected has some attractive properties.

Consider Figure 3(b) showing the required wing shape as a perturbation of the caret wing with the same leading edge which supports a plane shock wave in the plane of the leading edges and parallel flow over the surface. Then we select this parallel flow as a reference flow so that results previously derived for perturbing parallel flows may be used, and in particular we observe that the perturbation chosen generates a shape which is the same as the thin wings discussed in Section 2. Thus equations (1) and (2), with the parallel flow as reference, can be used to give an estimate of the change in the pressure due to the perturbation. That is, we may write

$$p_l = p_r + \gamma p_r \frac{M_r^2}{\beta_r} \frac{\sin a}{\sin b} \delta \tag{9}$$

$$p = p_r + \gamma p_r \frac{M_r^2}{\beta_r} \frac{\sin a}{\sin b} \delta (t_1 + t_2). \tag{10}$$

These equations could be in error because the parallel flow used as reference flow is bounded upstream by a shock wave and the effect of reflections from this shock wave has not been included. An analogous difficulty has been investigated[3] for a small change δ in the incidence of a two-dimensional wedge. The modification to the pressure in the flow behind the shock wave is found in this case to involve a term (λ) representing the attenuation of a disturbance on reflection from the shock wave. That is[3]

$$p_w = p_r + \gamma p_r \frac{M_r^2}{\beta_r} \delta \left(1 + 2 \sum_{n=1}^{\infty} \lambda^n \right) + O(M_r^2 \delta^2). \tag{11}$$

For shock waves not near detachment, $|\lambda|$ is less than 0.05 for $M \leqslant 5$. Thus the terms in λ are often small and may be neglected with the other non-linear terms. We assume, without theoretical justification, that other disturbances undergo a similar attenuation on reflection from the shock wave, and more specifically that the error terms for the wedge [i.e. in equation (11)] are similar to the neglected terms in equations (9) and (10). Subtraction of equation (11) from equations (9) and (10) gives

$$p_l - p_w = \gamma p_r \frac{M_r^2}{\beta_r} \left(\frac{\sin a}{\sin b} - 1 \right) \delta \tag{12}$$

and

$$p - p_w = \gamma p_r \frac{M_r^2}{\beta_r} \left(\frac{\sin a}{\sin b} (t_1 + t_2) - 1 \right) \delta. \tag{13}$$

Finally, as δ is constant over the wing, we can form, from equations (12) and (13), the non-dimensional pressure function

$$\frac{p - p_w}{p_l - p_w} = \frac{\sin a (t_1 + t_2) - \sin b}{\sin a - \sin b}. \tag{14}$$

This equation suggests that the function of pressure $(p - p_w)/(p_l - p_w)$ may be evaluated from the geometrical parameters, a and θ_l, and the reference flow value of b. Using equations (1), (2) and (8), equation (14) may be rewritten more simply as

$$\frac{p - p_w}{p_l - p_w} = \left(\frac{p - p_w}{p_l - p_w} \right)_{\text{thin wing}}, \tag{15}$$

whence the thick wing value of the pressure function may be obtained from a thin wing analysis of the surface.

The values of p_w and p_l on the left-hand side of equation (14) or (15) are obtained from oblique shock wave relationships[4] applied to the given wing. The values corresponding to the weaker of the two possible shock waves are used. On the right-hand side of the equation a and θ_l are obtained from the geometry of the wing, and b can be obtained as shown in Figure 2 from the extent of the leading edge region. That is, b is either obtained from the Mach number in the leading edge region through an equation equivalent to equation (5), or

from the position of R through a geometrical construction similar to that shown in Figure 2. These values differ from one another because the flow in the leading edge region is not necessarily parallel to the ridge line. Thus the region influenced by the nose of the wing is not a Mach cone centred on OO′, but a Mach cone centred on a line through O parallel with the flow direction in the leading edge region. For flows with large expansions near the centre of the wing the latter definition probably gives the better approximation. For wings with large compressions the formation of secondary shock waves in the flow tends to favour the former definition used here.

The pressure on the ridge line (OO′) is obtained by putting $\theta = 0$ in t_1 and t_2 [equations (3) and (4)] when equation (14) becomes simply.

$$\frac{p - p_w}{p_t - p_w} = \frac{b \sin a - a \sin b}{a \sin a - a \sin b}. \tag{16}$$

4. Comparison with Known Solutions

For the flat delta wing the pressure distribution has been obtained by several authors (eg, References 5 to 7) by numerical solutions to the exact equations. The pressure distributions computed by these methods do not fully agree with one another[5], particularly near the sonic cross flow point (i.e. the point labelled R in Figure 3 on the downstream Mach cone from the nose). The pressure distribution on a flat delta wing is obtained from the present method by putting $a = \pi/2$ and $\phi = 0$ in equations (3), (4) and (14) to give

$$\frac{p - p_w}{p_t - p_w} = \frac{2}{\pi} \frac{\tan^{-1}\{\tan b \,/\, (1 - \beta_1^2 \tan^2\theta)^{1/2}\} - \sin b}{1 - \sin b}. \tag{17}$$

The results from References 5 and 6 and equation (17) for a flat delta wing at Mach 4 are compared in Figure 4. The vertical axis shows the pressure coefficient and the horizontal axis shows a spanwise coordinate normal to the ridge line given by

$$y = \frac{\tan\theta}{\tan\theta_t}. \tag{18}$$

Thus $y = 0$ indicates the ridge line and $y = 1$ the leading edge. The pressure distributions are in close agreement except near the sonic cross flow point. At high Mach numbers the results[7] are as shown in Figure 5 for a flat delta wing at $M = 1000$.

In Figures 6(a) to (c) comparison between theoretical and experimental[8] values is shown for a caret wing of moderate anhedral over a range of Mach number and incidence. The results from the present theory can be seen to be close to the experimental values, and also close to Squire's theoretical[9] results except for occasional differences near the leading edge.

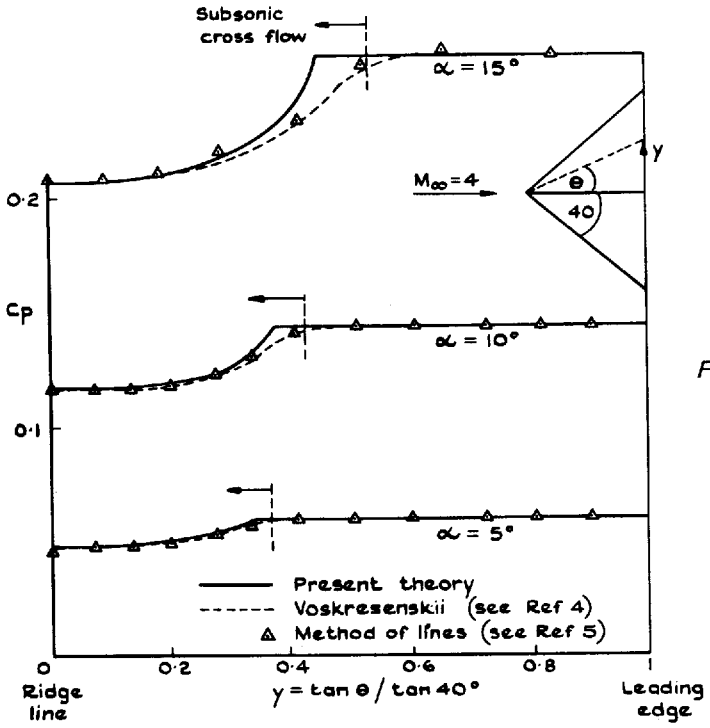

Figure 4 Pressure distribution on the lower surface of a flat delta wing at $M = 4$

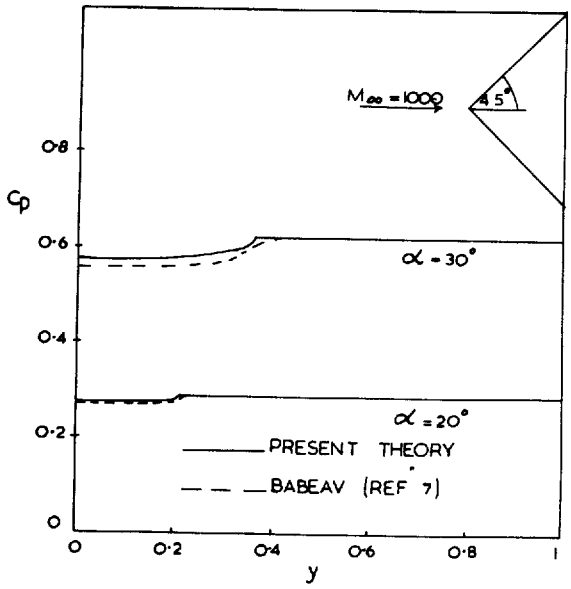

Figure 5 Pressure distribution on the lower surface of a flat delta wing at M = 1000

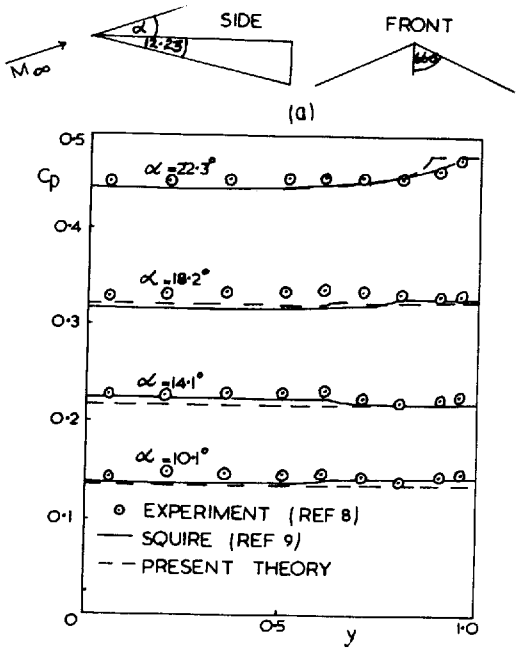

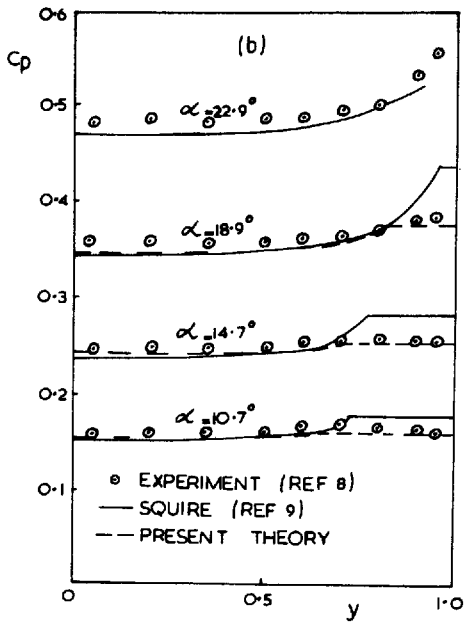

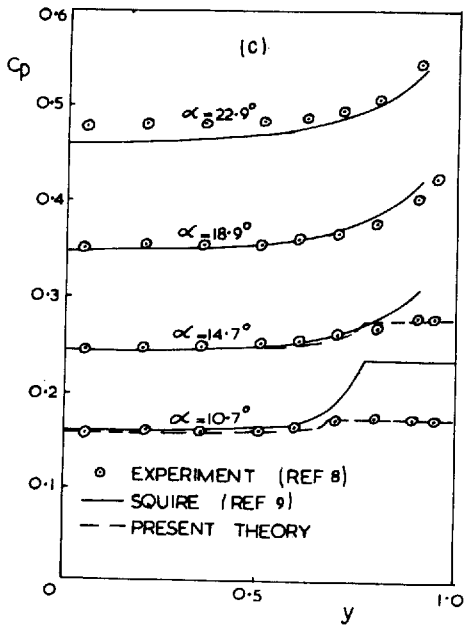

Figure 6 Pressure distribution on the lower surface of a caret wing
(a) M = 3.97
(b) M = 3.75
(c) M = 3.50

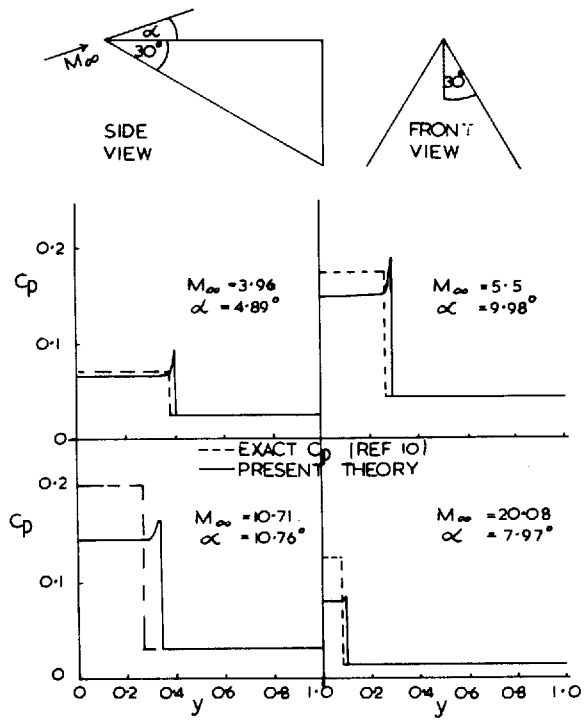

Figure 7 Pressure distributions on the lower surface of a wing of large anhedral

For wings of large anhedral Roe[10] has obtained some exact pressure distributions in which the flow is characterised by further shock waves in the flow behind the leading edge shock wave. In Figure 7 wings exhibiting large pressure changes in the flow are shown. It can be seen that, although the present theory is able to predict pressure coefficients accurately up to more than twice the leading edge value, larger pressure changes tend to produce errors. The pressure "spike" shown by the theory is the result of predicting some reflection of the second shock wave from the wing surface. Pressure distributions similar to this may actually occur for flow conditions which are close to Roe's crossed shock wave conditions shown. Further comparisons with exact and experimental results are presented in References 11 and 12. It is found in general that the errors are small for the lower surface except when large spanwise pressure gradients occur.

5. The Effect of Mach Number, Wing Anhedral and Leading Edge Sweep on the Pressure Distribution

Typical examples of the pressure distribution on the lower surface of a caret wing for various flow and geometry changes are shown in Figures 8 to 10. For a wing with $a = 62.5°$ and $\theta_l = 31.5°$ at an incidence of 10°, the pressure distributions for Mach numbers from 2.8 to 1000 are shown in Figure 8. The wing shape is indicated at the top of the figure. The pressure distributions show that at $M = 4$ the pressure is constant and the wing supports a plane shock wave. Above Mach 4 a compression occurs near the centre of the wing, possibly resulting in a second shock wave at very high Mach numbers. The ratio of specific heats is assumed to be 1.4 throughout. Thus the pressure distribution at $M = 1000$ is not representative of air flow. Some examples of the effect of γ on the pressure distribution are given in Reference 12. For Mach numbers below 4, the most significant feature is the high pressure region which develops near the leading edge when the shock wave is close to detachment. Near regions of large pressure change errors can occur in the predicted pressures; thus the pressure shown for $M = 2.8$ and for y about 0.8 to 0.9 is likely to be an overestimate.

The effect of changing the included angle between the wing panels or the anhedral of the same wing is shown in Figure 9. Front views of the wing with the appropriate pressure distributions are shown at the top of the figure. It can be seen that increasing the anhedral of this wing gives a compression at the wing centre, whilst decreasing the anhedral gives an expansion.

The average pressure coefficient or the lift coefficient of the wing with a streamwise upper surface is shown in the lower part of Figure 9, the lift coefficient of the constant pressure wing being taken as unit reference value. We observe that the lift coefficient for the constant pressure wing and the flat wing are approximately equal, but that intermediate amounts of anhedral result in lift coefficients which are better than either. It is found that in general a small improvement in the performance of caret wings can be obtained by halving the anhedral required for the constant pressure or plane shock wave condition.

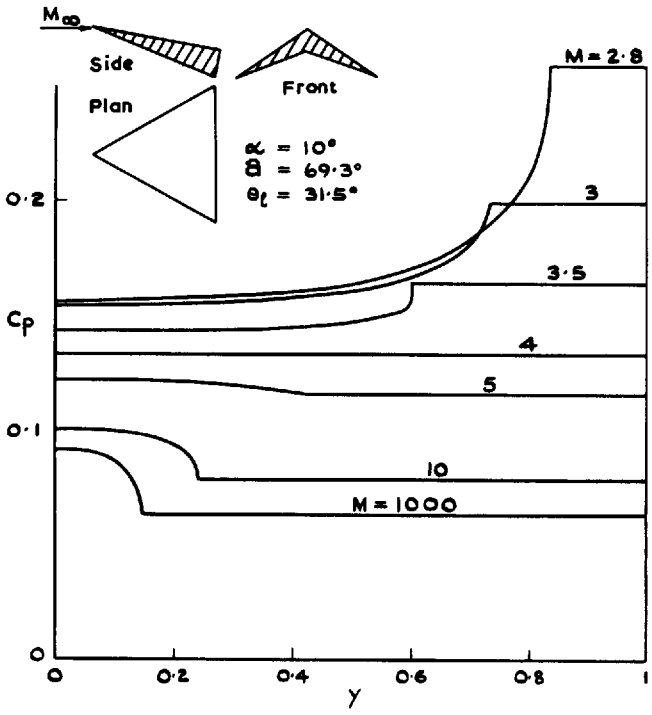

Figure 8 Pressure distribution on a caret wing for a range of Mach numbers

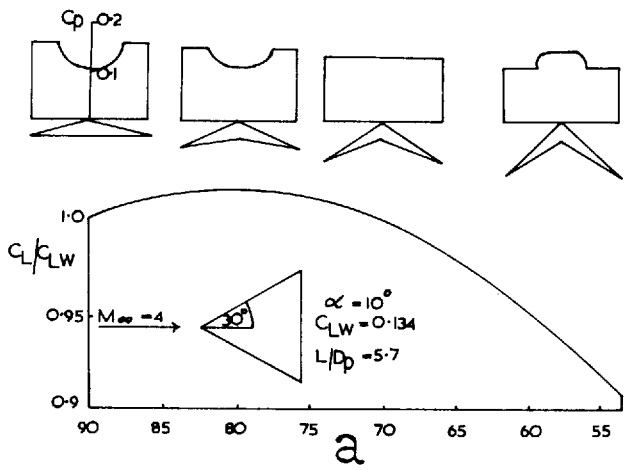

Figure 9 Pressure distribution and lift coefficient variation with anhedral

The change in pressure distribution with leading edge sweep is shown in Figure 10. The wings are formed by varying the nose panel angle (θ_l) of the wing used in Figure 8. Note that in Figure 10 the horizontal axis shows $\tan\theta$ rather than $y = \tan\theta/\tan\theta_l$ of the previous figures. Thus the pressure distributions have the same physical scaling for all the wings with the leading edge at $\tan\theta = \tan\theta_l$. A 1/10th scale front view of the six wings is shown at the top of Figure 10. For the unswept wing a significant pressure rise occurs near the "corner". Increasing the sweep increases the pressure near the leading edge and decreases the pressure inboard, whilst making very little difference to the extent of the inboard region. It is found in general that, except when the shock wave is close to detachment, the extent of the flow region influenced by both wing panels is insensitive to leading edge sweep.

6. Extension to Upper Surfaces

The upper surfaces of caret wings have $a \geqslant \pi/2$ and can be at positive or negative incidence to the free stream. For negative incidence p_l and p_w are determined from isentropic expansion values rather than shock wave compression values. Using these values of p_l and p_w, the pressure from equation (17) is shown to compare closely with the pressure on the upper surface of a flat delta wing[13] in Figure 11.

When the upper surface is at positive incidence p_l and p_w are obtained from shock wave values. The wedge incidence used to obtain p_w, however, is taken more generally to be the minimum angle between the free streamline through the nose and the surface. For the lower surface this corresponds to the ridge line incidence already used. For the upper surface at positive incidence the local panel incidence is then the equivalent wedge incidence for p_w, and the equation equivalent to equation (14) is given by

$$\frac{p - p_w}{p_l - p_w} = \frac{t_1 + t_2 - \sin b}{1 - \sin b}. \tag{19}$$

In Figure 12 the values from equation (19) are compared with experimental results[14] for $a = 99°$ and $M = 5.08$.

Although the comparisons made with known data are not as extensive for the upper surface as for the lower surface, it is clear that for some cases the theory provides an adequate estimate of the pressure distribution over the whole of the wing.

7. Conclusions

An expression is derived which relates the pressure in the supersonic flow past a wing to the pressure in the flow past a "thin" wing with the same surface shape. The expression is applied to caret and flat delta wings, with attached flow at their leading edges. It is suggested that it might have wider application to other wing shapes.

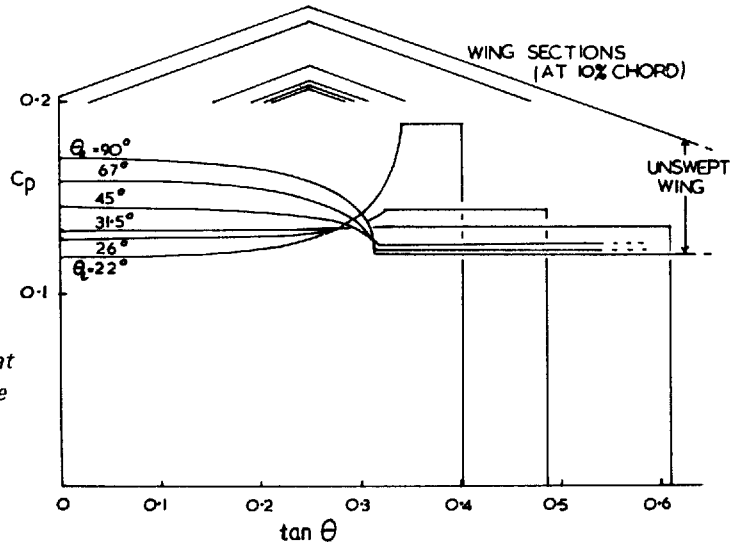

Figure 10 Pressure distribution on a caret wing at $M = 4$ *and* $\alpha = 10^\circ$ *for a range of leading edge sweep*

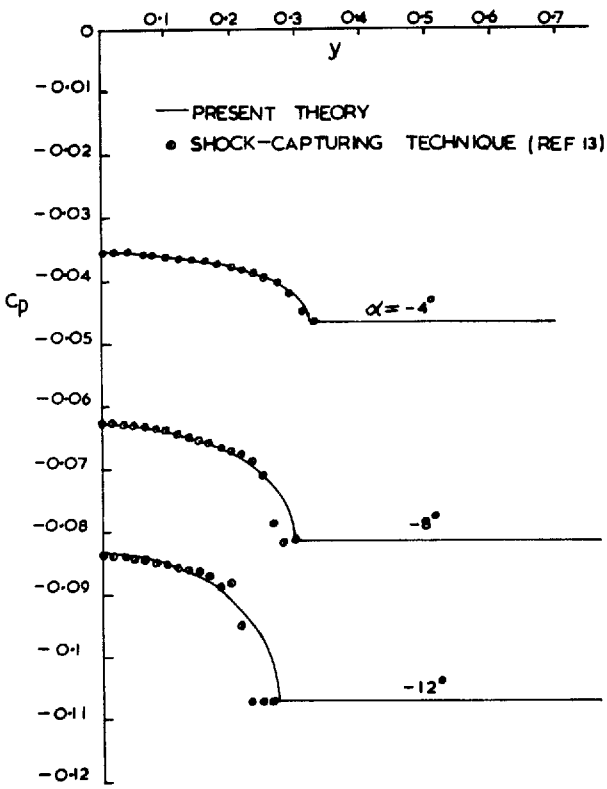

Figure 11 Upper surface pressures on a 45° swept delta wing at $M = 3$

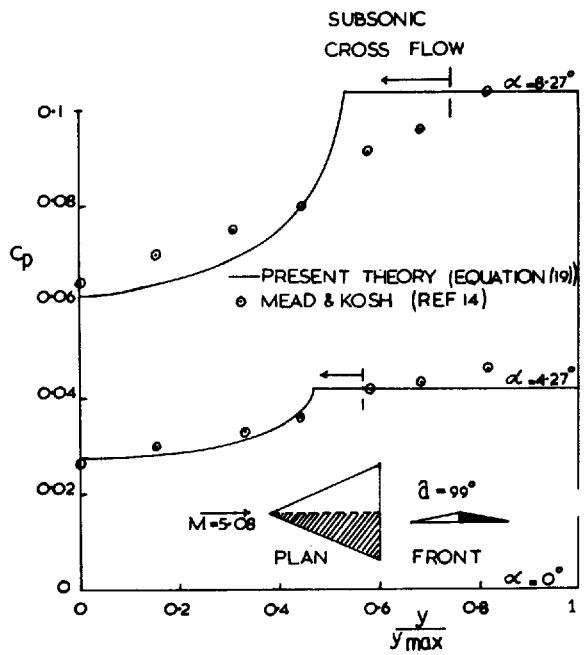

Figure 12 Upper surface pressures on a delta wing with $a = 99^\circ$

The "thin" caret and flat delta wing pressure distributions are obtained from an expression derived[2] using the well-known linear theory of supersonic flow. The resulting "thick" wing pressure distributions are found to be in good agreement with existing experimental and theoretical values, except when large pressure changes occur in the region behind the attached shock wave. Some expansion surface results are also obtained for wings with an isentropic expansion at the leading edge, but insufficient known results are available to assess the accuracy.

The effects of flow and geometry changes on the pressure distribution over a caret wing are investigated. using the method. It is found that near the leading edge a constant pressure region occurs, whilst inboard of this region expansions or compressions occur according to a simple pattern. The extent of this inboard region is sensitive to Mach number and incidence changes, but insensitive to changes in the leading edge sweep.

Lift coefficients are obtained by integrating the pressure coefficients. It is predicted that a small improvement in the lift/drag ratio can be obtained by halving the anhedral required for the plane shock wave condition.

References

1. T Nonweiler — Delta wings of shapes amenable to exact shock-wave theory. ARC 22 644, March 1961.

2. R M Snow — Aerodynamics of thin quadrilateral wings at supersonic speeds. *Quarterly of Applied Mathematics,* Vol V, No 4, 1947.

3. G G Chernyi — *Introduction to Hypersonic Flow.* Academic Press, 1961.

4. NASA-Ames Research Staff — Equations, tables and charts for compressible flow. NASA Report 1135, 1953.

5. J C South, Jnr, E B Klunker — Methods for calculating non-linear conical flows. NASA SP-228, 1969.

6. G P Voskresenskii — Numerical solution of the problem of a supersonic gas flow past an arbitrary surface of a delta wing in the compression region. Izv Akad Nauk SSSR, Mekh Zhid 1, Gaya 4, 1968.

7. D A Babaev — Numerical solution of the problem of supersonic flow past the lower surface of a delta wing. *AIAA Journal,* Vol 1, September 1963.

8. L C Squire — Pressure distributions and flow patterns at $M = 4.0$ on some delta wings. ARC R & M 3373, 1964.

9. L C Squire — Calculated pressure distributions and shock shapes on conical wings with attached shock waves. *Aeronautical Quarterly,* Vol XIX, pp 31-50, February 1968.

10. P L Roe — A special off-design flow for caret wings. Private communication.

11. J Pike — The flow past flat and anhedral delta wings with attached shock waves. RAE Technical Report 71081, April 1971.

12. J Pike — Theoretical pressure distributions on four simple wing shapes for a range of supersonic flow conditions. RAE Technical Report 71064, March 1971.

13. H Lomax, P Kutler — Numerical solutions for the complete shock wave structure behind supersonic-edge delta wings. *Third Conference on Sonic Boom Research.* NASA, Washington DC, October 29-30, 1970.

14. R M Mead, F Kock — Theoretical prediction of pressures in hypersonic flow with special reference to configurations having attached leading-edge shock. Grumman Aircraft Engineering Corporation, ASD TR 61-60, May 1962.